Deep Resources Engineering 2 (2025) 100165

Contents lists available at ScienceDirect

Deep Resources Engineering

journal homepage: www.keaipublishing.com/en/journals/deepre/

Full Length Article

Role of feature importance in geomechanical classification of rock slopes

Ashutosh Kainthola, Vishnu Himanshu Ratnam Pandey *, Gaurav Kushwaha, Vikas Yadav

Geoengineering and Computing Laboratory, Department of Geology, Banaras Hindu University, Varanasi 221005, India

ARTICLE INFO

Keywords:
SMR
Q-slope
GSI
Feature importance
Partial dependence
Economic Mitigations

ABSTRACT

Rock slope along motorways in the Higher Himalayan terrains are prone to various types of failure. In order to effectively mitigate these failures, a thorough assessment of rock mass behavior is entailed. The present research employs and compares widely practiced geo-mechanical classification schemes viz., RQD, RMR, SMR, Q-slope, and GSI. A 23 km road cut section, along Sangla to Chitkul route, in Higher Himalayan region (India) has been taken up for this work. Total of 18 locations were selected, and their slope and rockmass properties were examined. Afterwards, the most influencing parameters in RMR, SMR, and Q-Slope were evaluated through a machine learning algorithm, i.e., Random Forest. For $RMR_{basic,}$ about 83 % of rock-slopes were designated in *good* condition and rest were of *Fair* quality. Evaluation of slope mass rating along all 18-locations highlighted eight-sites as partially unstable, six-sites as partially stable. Remaining four locations varied between, *Very Bad* to *Bad* slope-conditions, necessitating the installation of mechanical supports and redesign of slopes. For SMR classification, feature importance analysis revealed the predominance of F3 variable, RQD and intact rock strength. Q-Slope approach was incorporated to identify the most stable steepest angle of the examined locations. For Q-Slope rating, J_n and RQD were found to have the most influence in classification of the slopes. Three zones on the basis of GSI-scores have been identified in the study area, i.e., A (65−95), B (45−55), and C (25−35). This study highlights the application of multiple geomechanical classification schemes, demonstrating how each approach can complement the others.

1. Introduction

Frequent slope instability disturbs the socio-economic dynamics of a nation [1–3]. Stability of rock-slopes is contingent upon the displacement along the discontinuities and the deformations in the intact rocks in varied stress-conditions [4–6]. Therefore, reliable joint parameters need to be carefully comprehended. Also, geometry, groundwater interactions, environmental conditions, freeze-thaw action, and seismicity have a considerable impact on the slope stability-conditions. Excavated rock-slopes in hilly terrains are at risk of failure, and require periodic geotechnical investigation and mitigation [2]. A trained engineering geologist integrates various engineering geological attributes at the site and decides the critical slope-angle, support-requirement, re-scaling, etc. Prevalent slope stability assessment techniques include, empirical, numerical, machine learning, remote sensing approaches [3,6,7]. However, empirical methods being simple-prompt-economic, are widely adopted.

Various empirical approaches emerged in the previous century to achieve safer developmental goals. Notably, Rock Quality Designation (RQD) [8], Rock Mass Rating (RMR) [9–11], Slope Mass Rating (SMR) [12–14], Q-Slope [15], Geological Strength Index (GSI) [16], Global Slope Performance Index [17], modified-GSPI [18], etc. Based on available resources and requirements, one or more methods can be used simultaneously. These techniques were successfully implemented in varied rockmass and geoenvironmental conditions across the globe [19–23]. Recently, a study [56] performed a comparative assessment using SMR and other practical approaches to solve the slope instability problems in Nainital district of Uttarakhand (India). Another work marks the usefulness of integrating artificial intelligence with the popular Q-Slope method to enhance the comprehension of slope failures in coastal regions [57]. A study identifies SMR as the most suitable geomechanical classification schemes incorporating inputs parameters, viz., slope height, rock mass heterogeneity, and discontinuity features [58]. Also, the Q-slope method has been validated as a reliable tool for slope stability assessment in Andean regions, demonstrating a robust accuracy and confirming its effectiveness across varied climatic conditions and

* Corresponding author.
E-mail address: pandey.vhr@bhu.ac.in (V.H.R. Pandey).

https://doi.org/10.1016/j.deepre.2025.100165
Received 20 November 2024; Received in revised form 29 January 2025; Accepted 2 February 2025
Available online 3 February 2025

failure modes [59].

Rugged Himalayan terrain poses numerous instability challenges [24–27]. Ansari et al. [28] performed comparable assessment of SMR and Q-slope along Devprayag and Srinagar Road. Siddique et al. [29] presented a correlation between Q-slope and CSMR to supports the suitability of the Q-slope method in Himalayan terrain. Khanna and Dubey [30] assessed road-cut slope stability in Himalaya using rock mass and discontinuity data from ten slopes. Dutta et al. [31] successfully evaluated slope failure issues in the Sikkim Himalaya by applying conventional SMR, Continuous SMR, Chinese SMR, and the Q-slope stability approach. Pandey et al. [32] implemented Q-slope and SMR along steep and critical slopes near Rishikesh town in Uttarakhand and the results were comparable to finite element techniques.

Frequent slope instability issues are observed in various parts of Himachal Pradesh each year, posing a significant threat to the development of the Himalayan state [33–35]. Accessibility to remote districts such as Kinnaur, Lahaul and Spiti, and Kullu is primarily dependent on roadways, as air and underground routes are limited. However, the challenging geoenvironmental conditions and complex geological setup exacerbate stability issues along these transportation routes [35]. These remote districts hold substantial economic and strategic importance for the nation, making all-weather connectivity crucial.

Several researchers have studied stability along these transportation corridors, but due to the diverse geotechnical behavior of rock masses and rapidly changing geological parameters, further investigation is needed [36]. Additionally, the abrupt variations in rock mass conditions necessitate a thorough understanding of the relative importance of classification attributes to enhance slope stability in a cost-effective manner [33,34]. Therefore, incorporating geomechanical classification for addressing instability issues, along with assessing feature importance and partial dependence of attributes is essential. The concept of feature importance and partial dependence has been unexplored for geomechanical slope attributes in empirical methods of stability analysis, making it a topic of potential interest for researchers and practicing geologists.

It is found that only a few recent researches have used these approaches to mark the key variables impacting different geotechnical phenomena. For example, a study [53] in 2024 created a model to identify important geological factors influencing tunneling operations and improve decision-making in similar tunneling projects. Another research [54] applied artificial intelligence, to predict lateral spreading resulting from soil liquefaction, concretely highlighting the most influential attributes in these enumerations. Also, the significance of data-driven approaches in geotechnical investigations is again demonstrated by the application of a machine learning technique to automatically extract important subsurface geological features [55]. When taken as a whole, these studies show how advanced computational methods can be integrated to evaluate the significance of features to guide accurate engineering choices.

Present study entails a comprehensive geotechnical field-investigation in Baspa valley of Kinnaur (Himachal Pradesh, India) to unzips the geomechanical classification parameters and facilitate the empirical stability analysis. These parameters aided the evaluation of geomechanical classifications namely RQD, RMR_{basic}, SMR, Q-Slope, and GSI. Kinematic analysis is an essential component of the study to assess any probable structural failure modes and complement the geomechanical classification schemes. Following which the attributes of RMR_{basic}, SMR, and Q-Slope were statistically examined to determine the feature importance on the particular scheme. Also, the effect of individual parameters on the ratings of classification were explored using partial dependence algorithms. Additionally, economic and effective mitigation measures were suggested based on RMR_{basic} and SMR. Ratings of Q-Slope were further used the assess the steepest possible slope without any robust-mechanical support, and highlights the need of rescaling at critical locations. The calculated GSI ratings indicated the pattern of rockmass quality along the studies road-section (23 km long).

2. Study Area

The study area is situated in the Higher Himalayan region, specifically in Sangla tehsil of Kinnaur district, Himachal Pradesh, India (Fig. 1). It can be approached from Shimla via National Highway 05 (NH-05), following the Satluj River to Karcham, where the Satluj and Baspa rivers converge, leading into the Baspa Valley. The terrain is marked by steep rocky cliffs and narrow roads alongside the Baspa River, with elevations ranging from approximately 2700 m to over 4000 m. The Baspa River, with its constant water-flow, powers two major hydroelectric projects located at Karcham and Kuppa. The local economy is largely based on apple orchards and tourism, with strategic significance due to the area's proximity to an international border.

Kharcham fault and Main Central Thrust have led a deteriorating impact on the physical and mechanical characteristics of the geomaterials. Active tectonic-setup in the region has made the area prone to seismic activity, further weakening the rockmass. Area belongs to the Vaikrita Formation, which dates back to the Eocambrian and Middle Cambrian periods, as well as the Haimanta Formations from the Early to Middle Proterozoic. The valley consists mainly of Kharo Gneiss from the Vaikrita Formation, with intrusions of Ordovician Kinnaur-Kailash Granite. Karcham Group of rocks includes quartzite, graphitic schist, psammitic gneiss, granitic gneiss, banded gneiss containing kyanite, and Rakcham Granite, all collectively known as granitic gneiss. Rakcham Granite forms part of the lower non-fossiliferous Haimanta Group from the Precambrian Era and is linked to the Vaikrita Group of the Proterozoic Era. Field observations reveal granitic-gneiss with alternating leucocratic and mesocratic bands.

3. Material and methods

Field-based datasets were used for comprehension of established rockmass classification schemes namely RQD, GSI, RMR_{basic}, SMR, and Q-slope. Required geomechanical parameters were carefully ascertained from 18 marked locations along Sangla-Chitkul route. At each precarious site discontinuity-orientations were documented using Brunton Compass. Joint-spacing, aperture, persistence, etc., were recorded with a measuring-tape. Infillings were carefully assessed. Barton's comb had aided the comprehension of 2-dimensional joint-roughness characteristics of joint-sets, and joint-roughness-coefficient (JRC) values were inferred as per work of Barton and Choubey [37]. In the field, Barton's comb was pressed against the joint surface to obtain imprints of representative joint roughness. These imprints were then transferred onto blank sheets and ultimately digitized (Fig. 2a). Joint roughness coefficient (JRC) values as per examined joint-roughness is a balanced distribution with a moderate spread (Fig. 2b). The JRC-density is highest around the range of 4–6, reflecting the most common values in the dataset. The presence of JRC-quartile lines within the violin plot indicates that a substantial portion of the data is concentrated around this median range, with fewer values deviating to the extremes. There are some outlier JRC-values at lower and higher ends, and majority of the JRC-datasets are clusters near the central region. This suggests that the JRC-datasets has a somewhat uniform distribution around the median, with moderate variability and no extreme skewness.

Presence of sheared rockmass were also examined for their impact on slope stability. Intact rock strength properties were addressed using a handy-tool during the field-survey, i.e., L-type Schmidth's hammer with impact energy 0.735 Nm. A schematic illustration of Schmidth's hammer working principle to gain rebound number value presented in Fig. 3a. Mathematically, the Schmidt hammer rebound number helped in understanding the intact rock strength values using the curves displayed on the tool. Analysis of rock strength values shows a relatively normal distribution centered around a mean of 54.33 MPa. The box plot indicates most values lie between 50 and 60 MPa with no significant outliers (Fig. 3b). And, histogram confirms this uniform distribution, suggesting consistent rock properties across the locations (Fig. 3c).

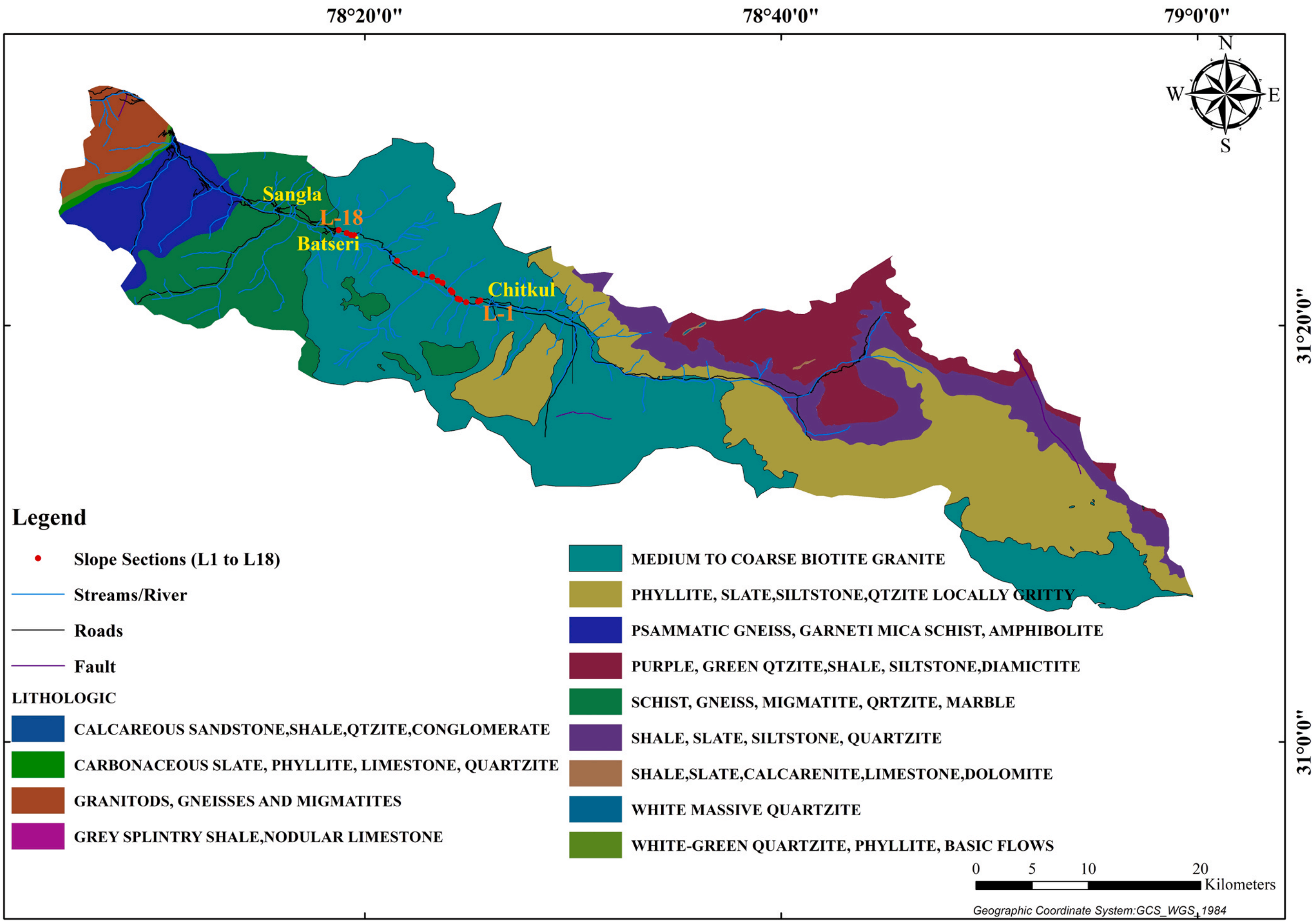

Fig. 1. Geological set of the study area with depicted critical slope sections along Sangla-Chitkul road. The study locations along the road are indicated by red dots, starting from Chitkul (L1) and extending to Sangla (L18) (Source: Geological Survey of India).

All these field-based datasets collected during field-investigation aids the geomechanical classification of rock-slopes and consequent rating for different schemes for each location were calculated. After evaluating the rating for geomechanical classification schemes, random forest algorithms were used to assess the feature importance and partial dependence plots for these respective schemes. In the present work, three geotechnical classification systems, namely RMR_{basic}, SMR, and Q-Slope were examined to determining their feature importance. As, to determine a rating value, each categorization scheme depends on particular input characteristics. Understanding how each parameter contributed to the final rating was the main goal of the analysis. Additionally, the random forest method can use metrics like Gini to calculate feature relevance.

In a similar manner, the Random Forest method was used to generate partial dependence plots (PDPs) in order to comprehend the impact of a particular attributes. This was assessed by varying one parameters of the given classification scheme while averaging the effects of others. This method provides interpretable insights into geotechnical classification systems by capturing intricate, non-linear linkages and interactions. These plots were effectively developed using a popular machine learning library, i.e., Scikit-learn.

3.1. Rock quality designation (RQD)

The degree of jointing and block size in a rockmass is an imperative parameter for development of any transportation corridors and other major infrastructural setups [38]. Some established methods dedicated in measuring the rock size are block volume (V_b), volumetric joint count (J_v), joint spacing (S), and RQD. The method for measuring block size depends on local conditions and the availability of measurement techniques. During the planning stage of any development project, when the rock surface is hidden by soil or weathering, methods like core drilling or geophysical surveys are used. In contrast, during construction, rock mass conditions can often be directly observed in cut-slopes, tunnels, mines, and shafts, enabling more accurate measurements. These different measurements of rock sizes (particularly, RQD and joint spacings) are being widely used in different rock mass classification schemes namely RMR, SMR, Q-Slope, etc.

So, the present work emphases on accurate and scientific determination of RQD at each location marked susceptible during field-observations. Deere [8] defined it as the proportion of rock-core sections exceeding 10 cm in length relative to the total core length (Eq. 1). And, based on RQD values 5-classes have been delineated: very poor (0–25 %), poor (25–50 %), fair (50–75 %), good (75–90 %), and excellent (90–100 %). Edelbro [39] have highlighted some limitations of the RQD, which are well known in core logging and rock engineering. For example, RQD is 0 when joint spacing is 10 cm or less, and 100 when it is 11 cm or more. Also, RQD does not account for core fragments under 10 cm, regardless of whether they are weathered or fresh rock. And, in one-dimensional measurements of RQD like scanline or bore-hole logs are quite susceptible to direction of measurements [40]. Therefore, other appropriate methods of RQD calculation were introduced based on joint-spacings or fracture density.

$$RQD = \frac{\sum Length\ of\ core\ pieces > 10cm\ length}{Total\ core\ run} * 100 \tag{1}$$

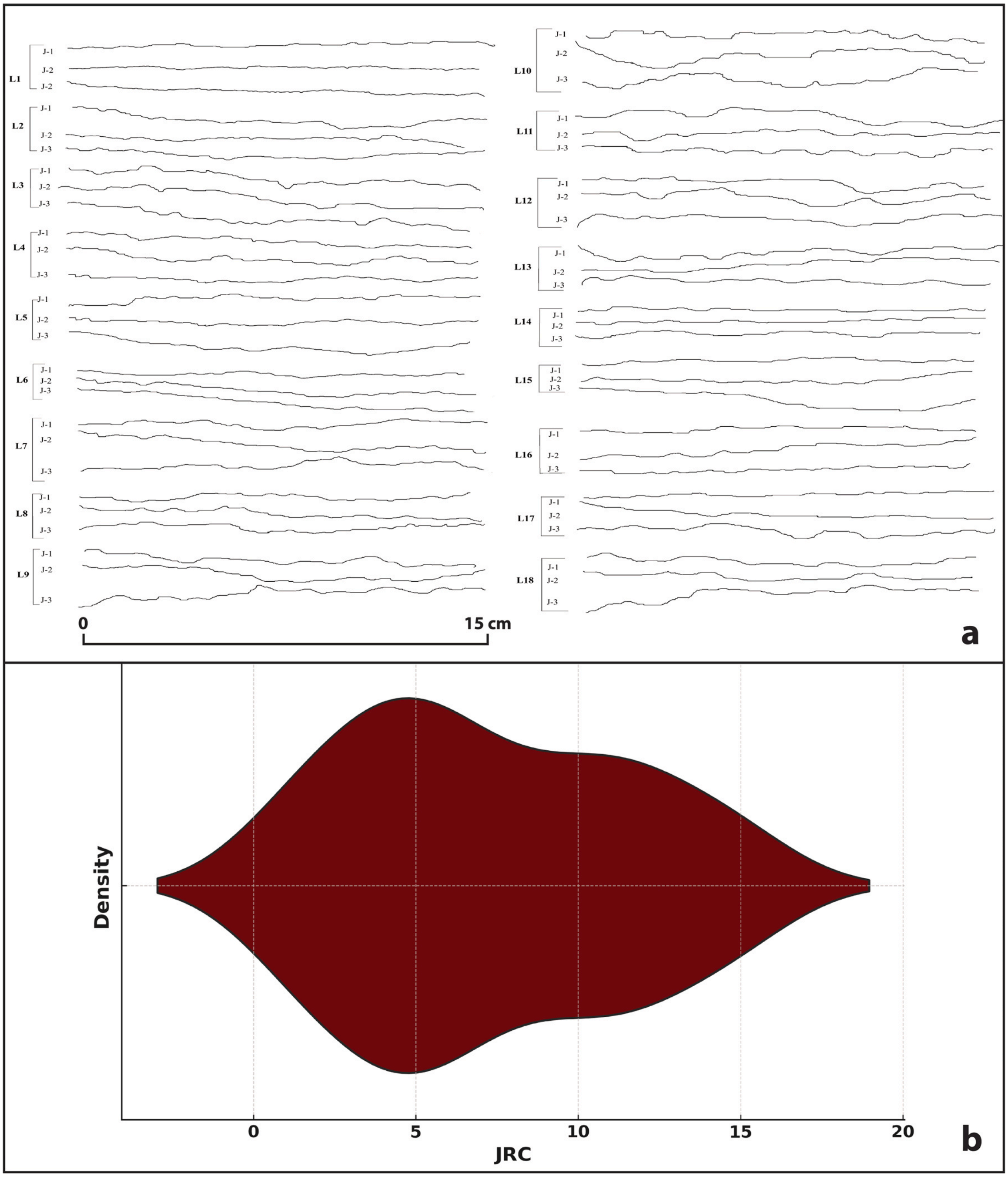

Fig. 2. (a) Roughness profile (15 cm) of natural joints ascertained using Barton's comb during field-investigation at each investigated location; **(b)** Joint Roughness Coefficient distribution pattern in the study area.

Palmstrom [38] derived a joint-spacing based RQD determination approach (Eq. 2), only applicable, when J_V varies in between 4.5 and 35. Otherwise, RQD is 0 in case J_V is more than 35 and RQD is 100 for J_V< 3.5. Later on, this equation was further refined as Eq. (3). The term J_V refers to volumetric joint count and enumerated mathematically using joint-spacing (S) between different joint-sets via Eq. (4).

$$RQD = 115 - 3.3J_V \quad (2)$$

$$RQD = 110 - 2.5J_V \quad (3)$$

$$\frac{1}{J_V} = \frac{1}{S_1} + \frac{1}{S_2} + \frac{1}{S_3} + \ldots + \frac{1}{S_n} \quad (4)$$

Similarly, mathematically established a viable relationship between RQD and joint frequency (Eq. 4). In the present work, RQD based on Eq. (2) has been derived for further analysis.

3.2. Kinematic Analysis

The rockmass usually consists of various structural fabrics (joints, foliations, beddings, etc.) bounding the intact rocks. Sometimes, the rock-cut slopes are contingent to structural failures owing to presence of unfavorably oriented discontinuities [41,42]. These discontinuities are mainly defined by attributes namely spacing, roughness, infillings, persistence, aperture, orientation, etc. And, all these factors along with strength of intact rocks greatly influence the cut-slope stability [42]. Among, these the orientation of structural-breaks, in conjunction with

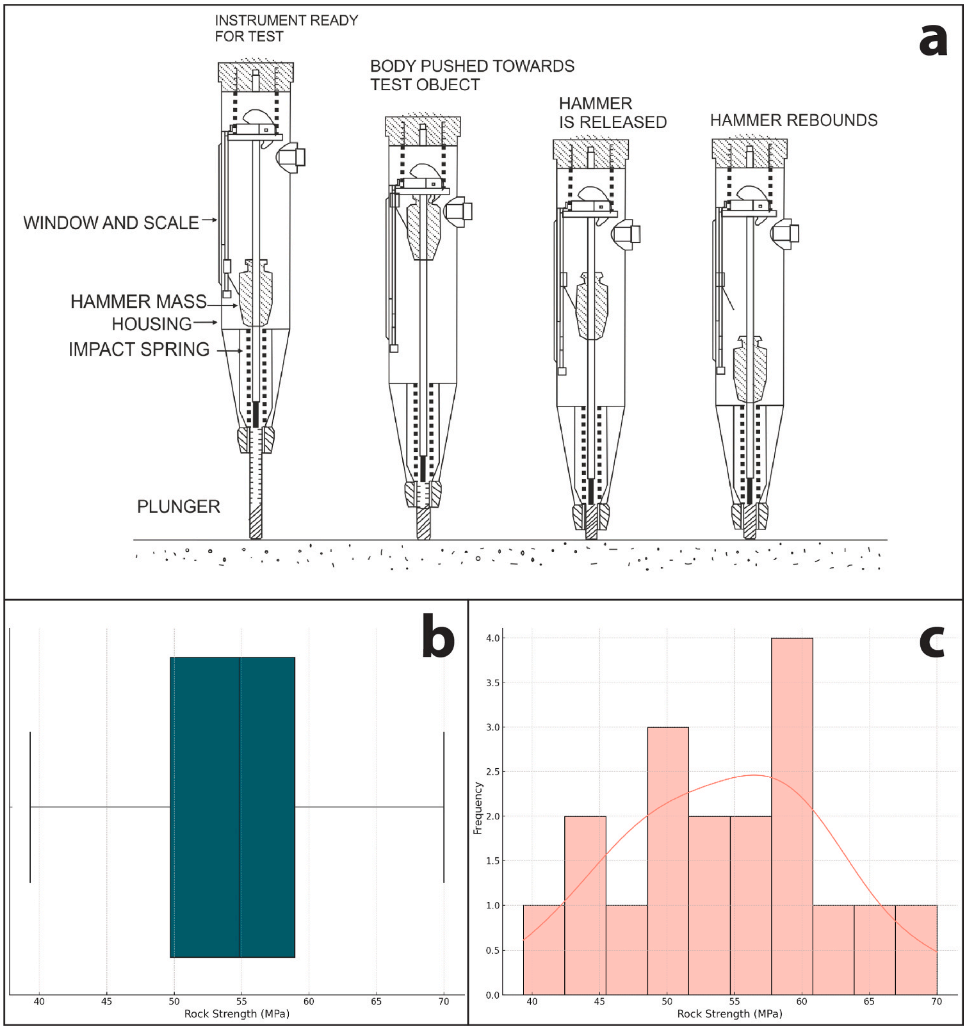

Fig. 3. (a) A schematic representation of working mechanism of Schmidth's Hammer; **(b)** distribution of intact rock strength values derived from Schmidth's Hammer test performed in field-investigation.

slope geometry, plays a dominant role in controlling the kinematic movement along these asperities in rock slopes [42]. Mainly, three-possible modes are outlined: planar, wedge, and toppling [42]. Toppling failures are further classified into flexural toppling and direct toppling [41]. Furthermore, in case of numerous discontinuities are present case of circular failure arises [41]. Various modes of kinematic sliding observed during the field-investigation are depicted in the Fig. 4.

Planar failures occur when a single discontinuity surface dips out of the slope face [32]. Wedge failures involve a mass of rock defined by two intersecting discontinuities, where the line of intersection is inclined out of the slope face [32]. Toppling failures happen when rock slabs or columns, defined by steeply dipping discontinuities into the slope face, topple forward. Circular failures are typical in rock masses that are either extensively fractured or consist of materials with low intact strength.

The kinematic analysis deals with examining the inherent discontinuity database over the slope's geometrical aspect considering the angle of internal friction. These planar structural features are plotted on stereographic plots and based on certain rules probability of different modes of failures are comprehended in rocky slopes. Hoek and Bray [41] defined different set of conditions based on combination of features such as slope face dip, slope face dip-direction, joint dip, joint dip-direction, friction angle on the joint, and plunge of joint-intersections.

3.3. Rock mass rating (RMR)

The rock mass classification schemes are considered an intuitive and handy mean to comprehend the rock mass conditions, active stresses, and hydrological control at a project-site during the initial stage. Several practitioners, engineers, and geologists with their plethora of experience at multiple project locations across the globe attempted to reach a common consensus to classify rock mass [9,11,15,43–47]. The main hurdle was to decide the influencing parameters to considered and their weightage.

Rock mass rating (geomechanical classification) introduced by [9] and refined with further inputs from multiple case histories and expert's suggestions [11]. This was the first broadly recognized rock mass classification system designed to quickly assess rock mass strength using six parameters: intact rock compressive strength (UCS test/ Schmidth's Hammer readings), Rock Quality Designation (RQD), discontinuity spacing (DS), discontinuity conditions (DC), groundwater conditions (GwC), and discontinuity orientations. The discontinuity conditions are based on the assessment of joint-roughness, infilling, aperture, weathering, persistence, etc. Bieniawski [11] assigned ratings to each of the six parameters mentioned, and these ratings are then summed to determine the RMR-value. The final RMR ratings are categorized into five rockmass classes: very poor (less than 21), poor (21–40), fair (41–60), good (61–80), and very good (81–100). In the present work, following the guidelines of Bieniawski [11] each parameter is examined (excluding

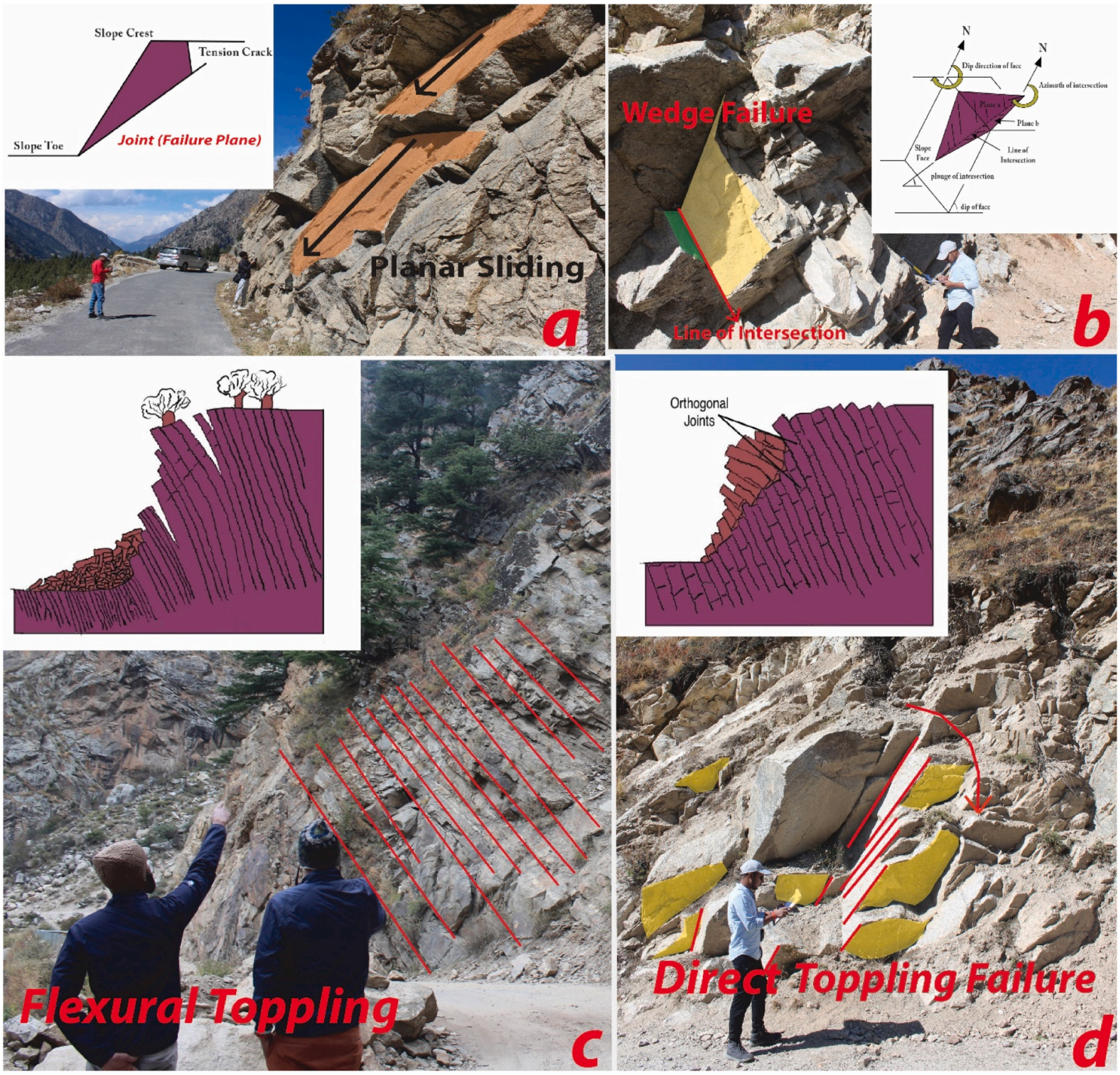

Fig. 4. Different modes of structurally-controlled failure situations observed during field-survey: **(a)** planar sliding, **(b)** wedge failure, **(c)** flexural toppling, and **(d)** direct toppling.

Table 1
RMR_{basis} ratings for each parameter based on Bieniawski [11].

Locations	Strength of intact rock (Schmidth's Hammer)	RQD	Joint Spacing	Condition of Discontinuities	Groundwater Condition	RMR_{basic}
L1	7.00	13.00	10.00	15.00	15.00	60.00
L2	4.00	20.00	10.00	15.00	15.00	64.00
L3	4.00	20.00	20.00	17.00	15.00	76.00
L4	7.00	20.00	10.00	20.00	15.00	72.00
L5	7.00	20.00	15.00	12.00	15.00	69.00
L6	7.00	17.00	10.00	14.00	15.00	63.00
L7	7.00	20.00	8.00	13.00	15.00	63.00
L8	4.00	17.00	15.00	10.00	15.00	61.00
L9	7.00	20.00	20.00	14.00	15.00	76.00
L10	7.00	20.00	20.00	12.00	15.00	74.00
L11	7.00	20.00	15.00	8.00	15.00	65.00
L12	7.00	17.00	15.00	12.00	15.00	66.00
L13	7.00	20.00	15.00	16.00	15.00	73.00
L14	7.00	17.00	15.00	8.00	15.00	51.00
L15	7.00	8.00	10.00	15.00	15.00	55.00
L16	7.00	13.00	10.00	16.00	15.00	61.00
L17	4.00	17.00	10.00	9.00	15.00	55.00
L18	7.00	17.00	15.00	8.00	15.00	62.00

the discontinuity-orientation) to evaluate RMR_{basic}. Additionally, the derived RMR_{basic} will be further included to assess the slope mass rating in this work, as discussed in next sub-section. Table 1

$$RMR_{basic} = \sum (rock\ strength + RQD + DS + DC + GwC) \tag{5}$$

3.4. Slope mass rating (SMR)

SMR is a rock mass classification system explicitly tailored for evaluating the instability of slopes. Romana [12] suggested incorporation of some additional factors F_1, F_2, F_3, and F_4 in RMR_{basic} [11]. These attributes account for the orientation of discontinuities relative to the slope face and excavation method (Eq. 6). SMR is mainly valuable in the field of geotechnical engineering for designing and evaluating engineered (or natural) slopes, such as highway cuts, mining operations, and other construction projects in rocky terrains. It helps engineers to predict potential failure modes and implement appropriate stabilization measures. Table 2 illustrates attributes contributing in SMR evaluation corresponding to each location. Correlation is also drawn among the SMR variables and its score pertaining to the present research (Fig. 5). The heatmap highlights the relationship between various geotechnical parameters and the Slope Mass Rating (SMR), revealing key insights into their influence. Among the features, DS and RQD show a moderate positive correlation with SMR. Additionally, F4 exhibits a strong positive correlation, making it the most impactful parameter for SMR assessment, while discontinuity condition has a weaker yet positive relationship. These observations emphasize the importance of DS, RQD, and especially F_4 in geotechnical evaluations related to Slope Mass Rating Scheme.

The classification ranges from very good to very poor stability, guiding design decisions and slope management strategies. By incorporating geological, geometrical, and mechanical aspects, the SMR system provides a comprehensive framework for slope stability analysis, which is essential for safe and cost-effective slope design and management [14,48].

$$SMR = RMR_{basic} + (F_1 \times F_2 \times F_3) + F_4 \tag{6}$$

3.5. Q-Slope

Q-Slope is a rock-slope stability classification system modified from the Q-System, originally developed by Barton et al. [15] to assess rock mass quality in underground works. Q-Slope adapts the Q-System specifically for slope stability analysis, incorporating parameters that are crucial for evaluating rock slopes. This system provides a quick and reliable method for assessing the stability of natural and excavated slopes, such as those found in road cuts, open-pit mines, and other geotechnical settings.

Q-Slope is chiefly beneficial in the primary stages of project planning, serving engineering geologists to demarcate potential failure modes, design slope geometry, and recommend robust-economic stabilization measures. It's practically-handy use allows for prompt classification and decision-making, employing familiar rock mass parameters. This organized method is flexible to the numerous geological conditions, making it an intuitive and viable instability assessment method. The assessment of Q_{slope} to examine slope instability is based on RQD, joint-set number (J_n), joint-roughness number (J_r), joint-alteration number (J_a), environmental and geological conditions (J_{wice}), and slope strength reduction factor (SRF_{slope}) mathematically arranged as in Eq. (7). Also, the concept of orientation factor is introduced in shear-strength parameter (J_r/J_a) of original Q-system, and based on planar or wedge sliding these orientation factors are multiplied in Eq. (7) [49].

$$Q_{slope} = \frac{RQD}{J_n} \times \left(\frac{J_r}{J_a}\right)_O \times \frac{J_{wice}}{SRF_{Slope}} \tag{7}$$

Q-Slope is particularly useful for providing guidance on steepest slope angles for different slope condition based on the work of Barton and Bar [49]. It aids in ensuring that slopes are designed within safe limits, thereby reducing the risk of slope failure and enhancing the overall stability of rock slopes in engineering projects. This mathematical relationship between Q-Slope and steepest slope angle (β) is formulated in Eq. (8). Table 3

$$\beta = 20\log_{10}(Q_{Slope}) + 65 \tag{8}$$

The correlation matrix analysis (Fig. 6) reveals that parameters such as J_a and J_{wice} exhibit strong positive correlations with the Q-Slope value (0.67 and 0.72, respectively). This indicates that higher J_a values, which reflect more altered joints, and higher J_{wice} values significantly enhance slope stability. Conversely, J_n and the Slope Reduction Factor have negative correlations (-0.49 and −0.46), suggesting that an increase in these parameters leads to a reduction in slope stability. RQD and J_r show moderate positive correlations with Q-Slope, implying their effects on slope stability.

3.6. Geological strength index

The introduction RMR [9] and Q-system [15] proved useful in various practical application of geotechnical projects. However, their major dependence on RQD gave poor results for weak rock masses (RQD = 0) and yield proper solutions under moderate stress conditions. In late 1970s, Hoek and Brown realized that for a rock-mass failure criterion to be useful, it needed to be easily connected to geological observations that field geologists or engineering geologists could make quickly. Over the time, with rigorous research works involving hundreds of case studies and discussion with practicing engineering geologist idea of geological strength index (GSI) was first conceptualized by Hoek [16], and further revised in the present usable form [50–52].

This classification is easy to comprehend during the field-investigation on the basis of blockiness in the rockmass and surface conditions of the inherent discontinuities in them. It served as an excellent approach for estimating rock mass properties (as direct in-situ testing are unapproachable) by considering both the characteristics of intact rock and the nature of discontinuities in the rock mass, which could be applied in rock mass failure criteria.

4. Results and discussion

4.1. Rock quality designation

Deere [8] suggested five categories of rock quality ranging from excellent to very poor. On the basis of field-observations and

Table 2
Assessment of SMR parameters using field-data and kinematic analysis [12].

Locations	RMR_{basic}	F1	F2	F3	F4	SMR
L1	60.00	0.40	1.00	−25.00	0.00	50.00
L2	64.00	0.15	1.00	−25.00	0.00	60.25
L3	76.00	0.15	1.00	0.00	0.00	76.00
L4	72.00	0.70	1.00	−60.00	0.00	30.00
L5	69.00	0.85	1.00	−60.00	0.00	18.00
L6	63.00	0.15	1.00	−25.00	0.00	59.25
L7	63.00	0.85	1.00	−25.00	0.00	41.75
L8	61.00	0.15	1.00	−60.00	0.00	52.00
L9	76.00	0.15	1.00	−25.00	0.00	72.25
L10	74.00	1.00	1.00	−6.00	0.00	68.00
L11	65.00	0.85	1.00	−6.00	0.00	59.90
L12	66.00	0.15	1.00	−25.00	0.00	62.25
L13	73.00	1.00	1.00	−6.00	0.00	67.00
L14	51.00	0.15	1.00	−25.00	0.00	47.25
L15	55.00	0.70	1.00	−50.00	0.00	20.00
L16	61.00	0.70	1.00	−6.00	0.00	56.80
L17	55.00	0.15	0.85	−60.00	0.00	47.35
L18	62.00	0.70	1.00	−60.00	0.00	20.00

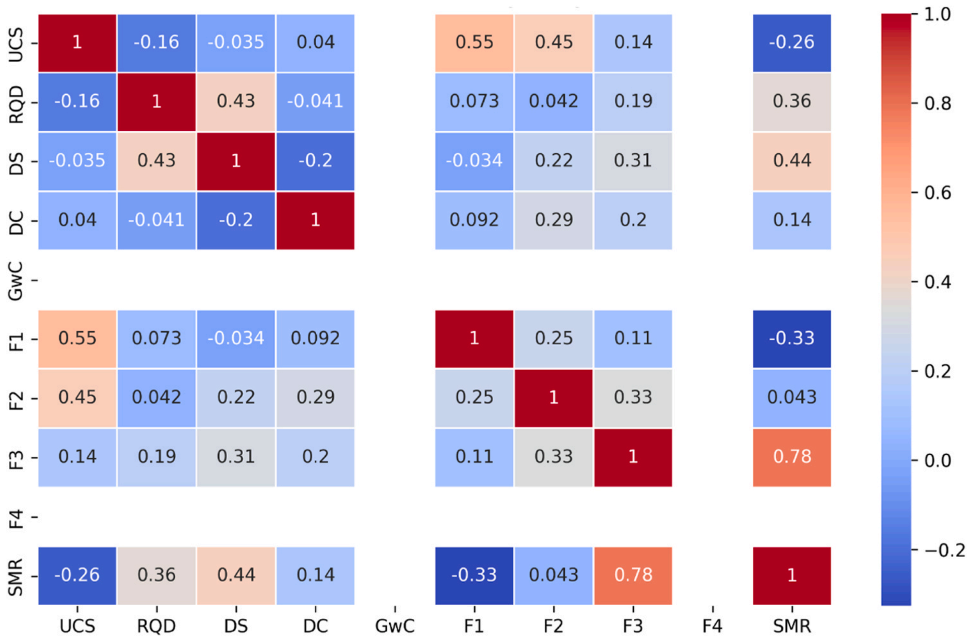

Fig. 5. Correlation matrix of the features pertaining to SMR analysis.

Table 3
Q-Slope parameters inferred during field investigation.

Locations	RQD	J_n	J_r	J_a	J_{wice}	SRF_{slope}	O-factor 1	O-factor 2	Q-Slope
L1	73.0	6.00	4.00	6.00	0.30	5.00	0.75	NA	0.37
L2	94.60	9.00	3.00	4.00	0.30	2.50	0.75	0.68	0.48
L3	96.20	9.00	3.00	3.00	0.90	5.00	1	NA	1.92
L4	85.00	6.00	3.00	1.00	0.30	2.50	0.75	NA	3.83
L5	92.00	9.00	3.00	3.00	0.30	2.50	0.75	NA	0.92
L6	97.50	9.00	1.50	1.00	0.30	2.50	0.75	NA	1.46
L7	89.00	12.00	3.00	8.00	0.30	5.00	0.75	NA	0.13
L8	98.40	9.00	1.00	1.00	0.30	2.50	0.75	0.9	0.89
L9	97.30	9.00	3.00	2.00	0.30	2.50	0.75	1.35	1.97
L10	98.40	12.00	4.00	2.00	0.30	2.50	0.75	1.8	2.66
L11	89.70	9.00	3.00	2.00	0.30	5.00	0.75	NA	0.67
L12	84.00	9.00	3.00	2.00	0.30	10.00	0.75	NA	0.32
L13	96.60	9.00	3.00	0.75	0.30	10.00	1	NA	1.29
L14	92.00	9.00	3.00	2.00	0.30	2.50	0.75	NA	1.38
L15	76.00	9.00	3.00	2.00	0.30	2.50	0.75	NA	1.14
L16	92.00	9.00	3.00	1.00	0.30	7.50	0.75	NA	0.92
L17	87.50	9.00	3.00	3.00	0.30	10.00	0.75	0.9	0.20
L18	91.70	15.00	3.00	2.00	0.30	5.00	0.75	1.35	0.56

joint-spacing datasets, the discerned RQD values are chiefly grouped in three different classes (Fig. 7). About 60 % studied sites (L2, L3, L5, L6, L8, L9, L10, L13, L14, L16, and L18) were of significant quality and termed as excellent category as their RQD value ranges in between 90 % and 100 %. Six-locations namely L4, L7, L11, L12, L15, and L17 were grouped as good rock class ($75 < RQD < 90$). Only, remaining L1 was determined to be in fair category with RQD value of 73 %.

4.2. Kinematic analysis

Kinematic analysis suggests that nearly all the sites (except L3) are prone to one or combined mode of structurally-induced failures. Wedge and direct toppling failure-modes are the most prominent and could affect 15 and 14 locations respectively. Nine locations are under the severity of planar sliding, and only 4 are prone to flexural toppling instability. The combination of failure types observed across the study locations indicates varying degrees of slope failure risk. For instance, L1 is predominantly prone to direct toppling, whereas L2 exhibits a combination of wedge and flexural-toppling. At L4, L5, L6, and L10 a combination of planar, wedge, and direct toppling failures are present, indicating a diverse risk profile. Location L7 shows a combination of wedge, flexural-toppling, and direct-toppling. Sites L8 and L12 have equal intensities of wedge and direct toppling instabilities. Location L9 is characterized by a dominant direct toppling risk with influence of flexural-toppling mode. At investigated site L11, there is a more complex mix involving planar, wedge, and direct-toppling. The analysis underscores the diverse geomechanical behavior of these sites, with different locations exhibiting distinct failure combinations (Fig. 8) and intensities, thus necessitating targeted mitigation strategies for each.

4.3. Rock mass rating (RMR_{basic})

Feature importance analysis for the RMR_{basic} parameters indicates that RQD is the most significant contributor to the RMR_{basic} score, followed by discontinuity spacing and discontinuity conditions. Intact-rock strength parameter has quite lower impact. Groundwater condition parameter being almost same for the entire study area has no contribution in feature importance analysis. The relative importance of RQD,

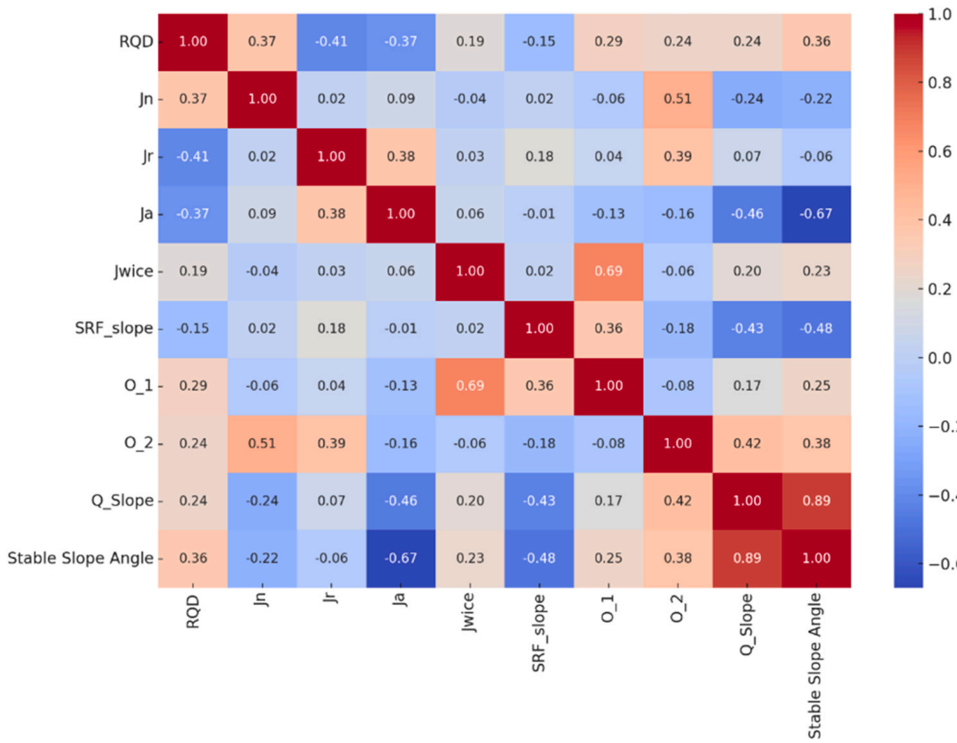

Fig. 6. Correlation matrix for the attributes utilized in Q-slope assessment.

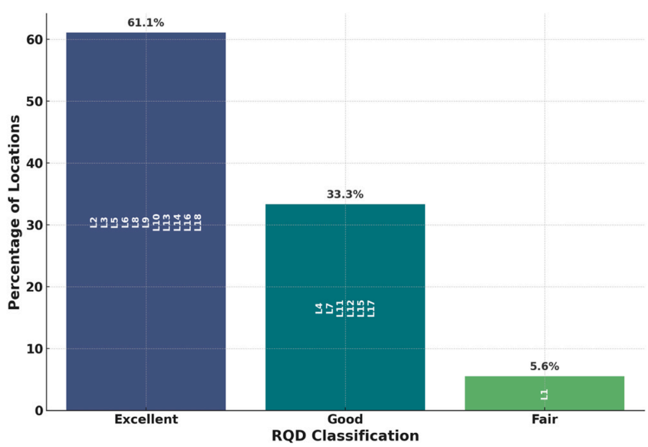

Fig. 7. Cluster of rock quality designation in the study area.

discontinuity spacing, joint conditions, rock strength, and groundwater is mapped to be 0.46, 0.31, 0.20, 0.03 and 0, respectively. So, prioritizing RQD and joint spacings will enhance RMR_{basic} ratings in the study area.

The partial dependence plot of RMR_{basic} reveal that higher rock strength, RQD, and wider discontinuity spacing (DS) positively influence the Rock Mass Rating, indicating stronger and more stable rock conditions (Fig. 9). Conversely, poor discontinuity condition (DC) and adverse groundwater condition (GwC) lower the rating, reflecting a negative impact on rock stability. These findings emphasize the critical role of these factors in evaluating rock mass quality for geotechnical applications.

The RMR_{basic} datasets calculated for the entire locations lies on two classes fair rock (41–60) and good rock (61–80). Only three locations namely L1, L15, and L17 belongs to fair rock quality based on RMR_{basic} ratings. And, remaining fifteen locations are grouped as good rock. For fair rock class locations, a systematic support installation is needed with regular monitoring and drainage control. And, in case of good rock quality a minor support such as rock bolts and attention to fractures will control the instability.

4.4. Slope mass rating (SMR)

Feature importance plot (Fig. 10) for classification parameters highlights that F3 is the most critical factor, contributing approximately 55.8 % to SMR's estimation. Discontinuity spacing (DS) and F1 also significantly impact the SMR, accounting for 14.2 % and 10.8 %, respectively. Rock Quality Designation and Discontinuity Condition (DC) have lower importance, indicating a relatively minor effect on SMR in comparison to F3. A negligible influence of groundwater condition (GwC), F4, and F2 is observed in the study area. On the basic of this analysis, a targeted interventions in important features like F3, DS, and F1 will significantly enhance slope stability condition and ease mitigation strategies.

Partial dependence plots for key SMR features reveal the influence of individual parameters on the SMR score while accounting for other variables (Fig. 11). Rock Strength shows a consistent positive relationship with SMR, suggesting that stronger rock improves slope stability. Similarly, an increasing trend in SMR is observed with higher RQD values, suggesting that better rock quality enhances slope safety. For discontinuity spacing (DS), the effect on SMR is moderate, reflecting a less pronounced impact. F3 has a notable non-linear effect. Therefore, the key parameters rock strength, RQD, and F3 should be thoroughly comprehended for improving the slope stability. Additionally, managing and optimizing the orientation of discontinuities is crucial. Addressing these parameters can effectively mitigate instability risks.

As per Romana [12] suggestions for SMR, the slope conditions are classified into five categories from completely unstable to stable. The majority of locations, including L1, L6, L7, L8, L11, L14, L16, and L17, fall under the "Normal" class of SMR and are partially unstable. Implementing mitigation strategies such as shotcrete, bolt anchors, toe ditches, and nets can significantly improve stability at these sites. Six locations, namely L2, L3, L9, L10, L12, and L13, are classified as having

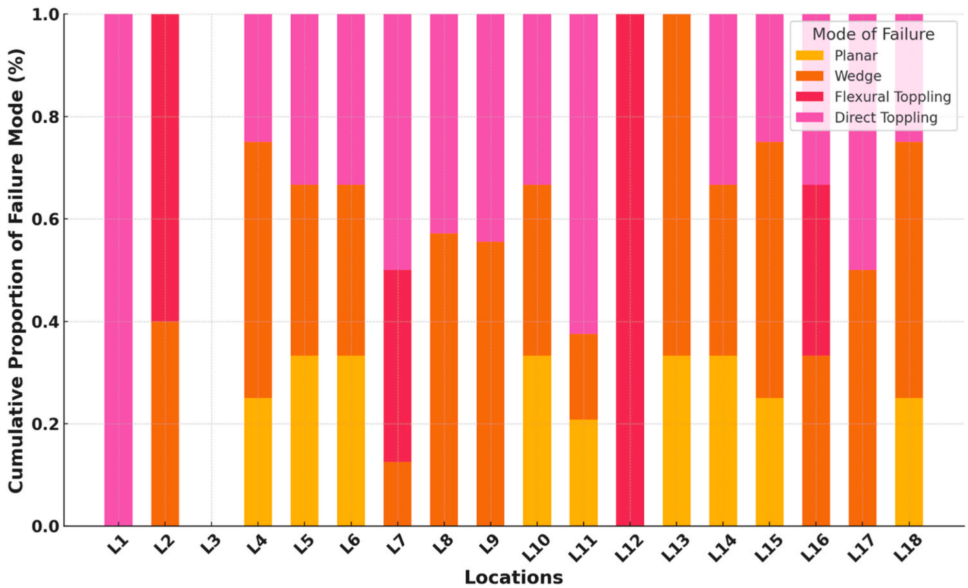

Fig. 8. The propensity of failure modes on the basis on percentage of joints involved in kinematic analysis.

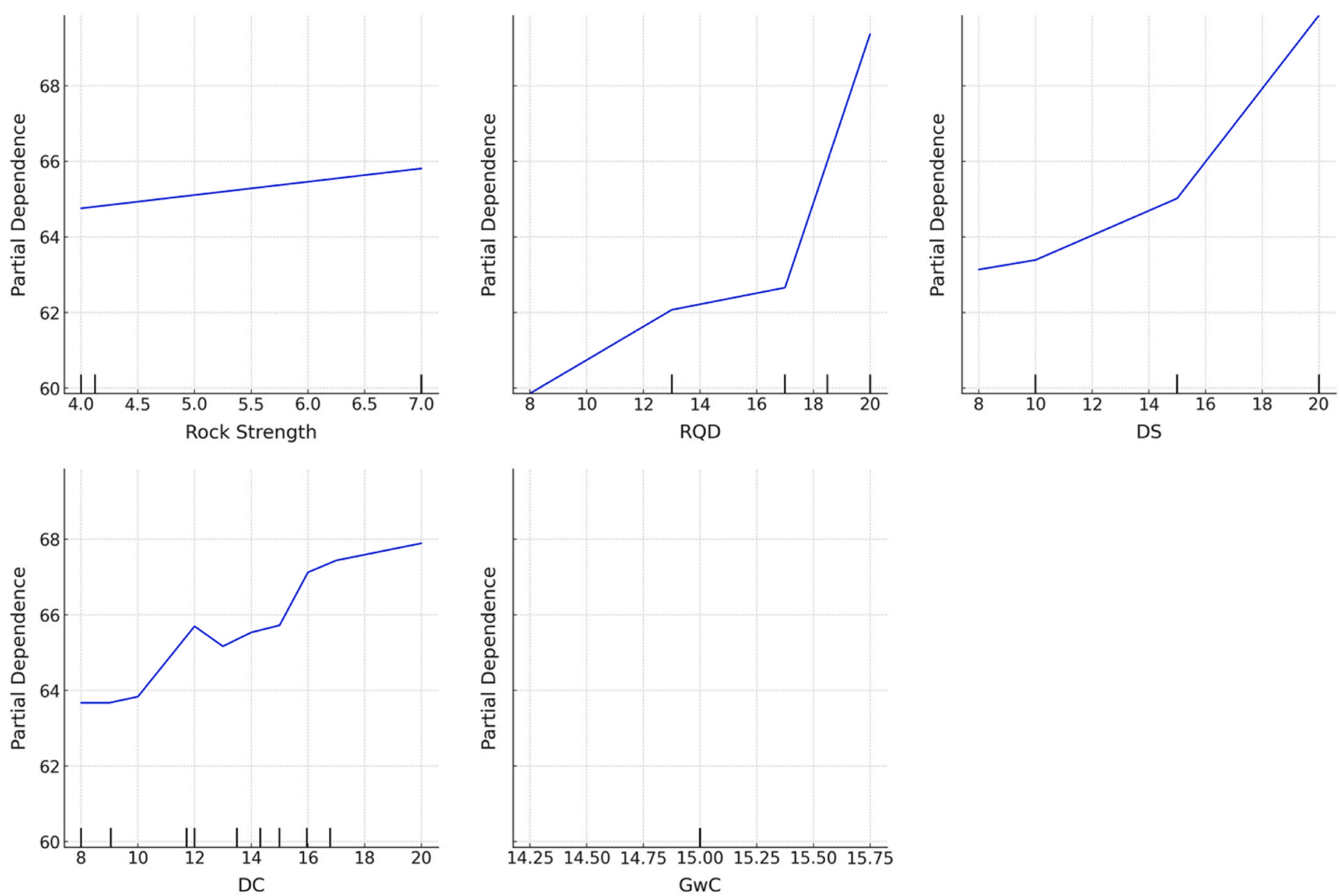

Fig. 9. Partial dependence plot for RMR_{basic} parameters on its rating.

a "Good" slope condition according to the SMR rating, indicating partial stability. Installing bolts, anchors, and fencing at these sites could further reduce risk. The "Very Bad" class includes three locations: L5, L15, and L18. These sites are completely unstable and require extensive measures such as re-excavation, drainage installation, shotcrete, and toe walls to enhance stability. Site L4 is categorized as "Bad" and would benefit from interventions like re-excavation, drainage control, concrete installation, and reinforcement techniques such as bolts and anchors. The mitigation strategies suggested are based on the work of Romana [12], as shown in the Fig. 12.

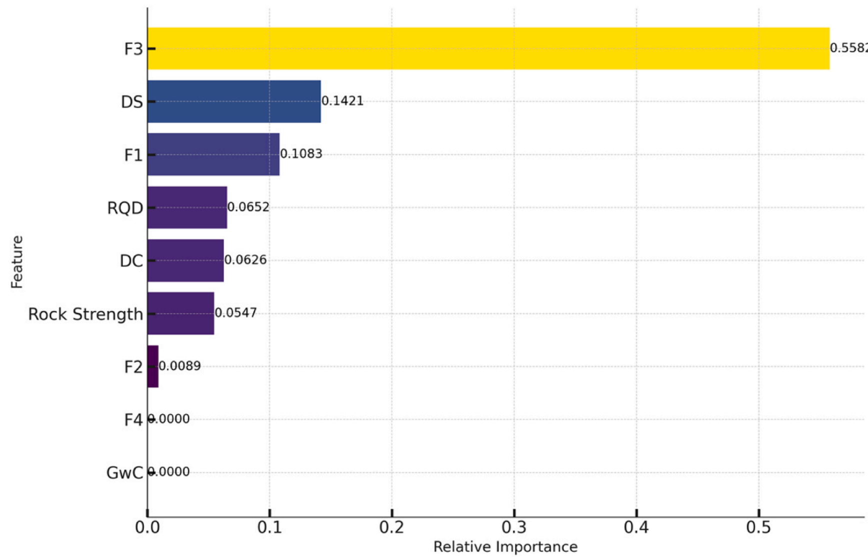

Fig. 10. Feature importance of SMR parameters in the present study area.

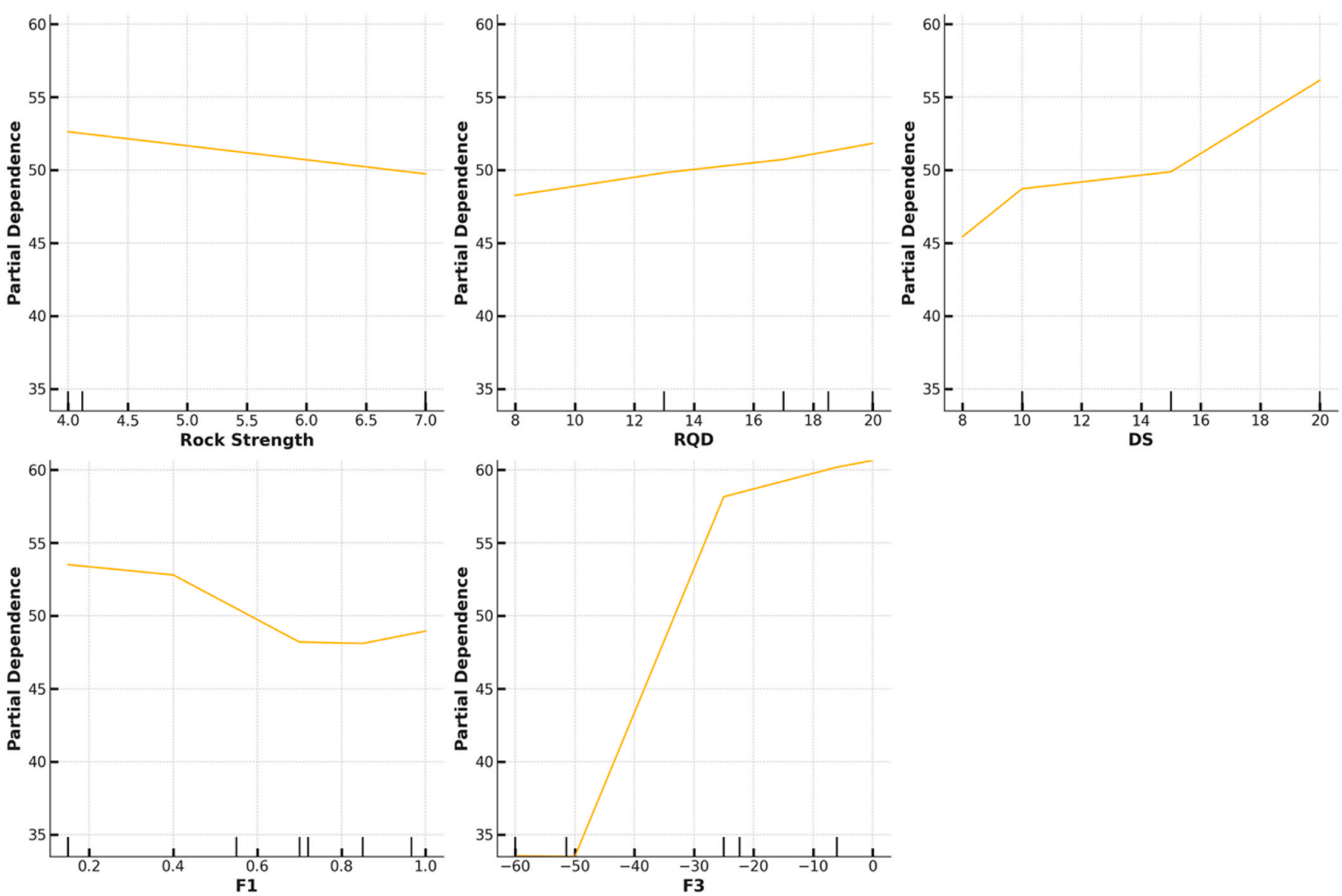

Fig. 11. Partial dependence plot for the key-features of SMR at the studied locations.

4.5. Q-Slope

An algorithm was developed to comprehend the feature importance in estimating Q-Slope (Fig. 13). Joint-set number and RQD termed out to be the top contributor with 29.95 % and 29.34 %, respectively. This highlights the critical roles that J_n and rock quality designation play in determining slope stability. Joint Roughness Number and SRF_{slope} also have notable, though lesser, influence, contributing 10.69 % and 9.69 %, respectively, indicating that joint roughness and slope reduction factors are of secondary importance. Orientation factor-2 adds 8.59 %, reflecting its moderate impact, while Ja and Jwice contribute 5.43 % and 3.90 %, showing even lower, though still relevant roles. Orientation factor-1 with only a 2.41 % contribution, has the least impact, suggesting its limited significance in the present study.

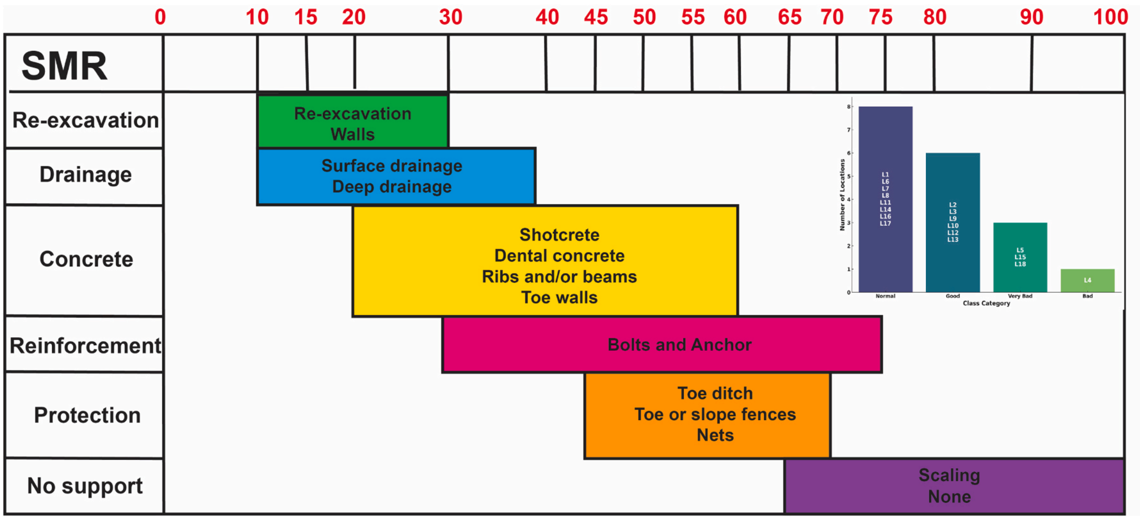

Fig. 12. Mitigation assessment for SMR ratings based on Romana [12].

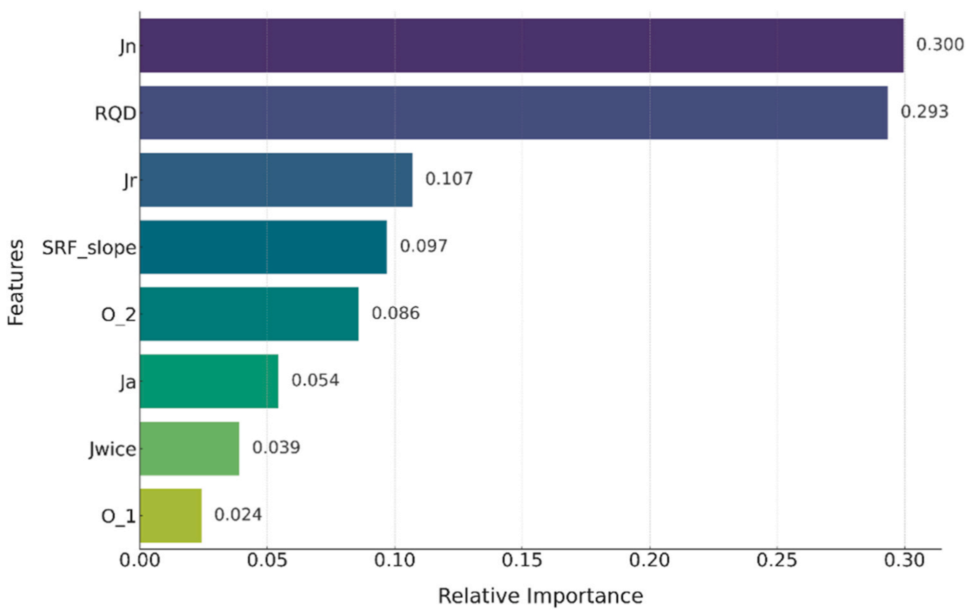

Fig. 13. Q-slope’s feature importance using random forest algorithm.

Partial dependence plots (PDPs) highlight the complex relationships of slope behavior under varying rock mass conditions (Fig. 14). RQD marks a strong positive correlation with Q-slope, particularly beyond an RQD of 90, indicating that superior rock quality significantly enhances stability. Joint-set number has a noticeable negative effect, with stability decreasing sharply as J_n rises from 6 to 10, after which the effect plateaus. Joint roughness number provides moderate improvement in stability, suggesting that rougher joints enhance frictional resistance. On the other hand, J_a and SRF_{slope} both show negative impacts, with Ja reducing stability as joints become more altered and SRF_{slope} leading to diminished stability, though its influence levels off at higher values. Meanwhile O-factor 2 exhibits a positive effect, pointing to the presence of favorable structural conditions. J_{wice} & O-factor 1 does not show the partial dependence relationship as these values are almost same for each location in the Baspa Valley. Together, these findings underscore the importance of optimizing rock mass characteristics to enhance slope design and mitigate risks in geotechnical engineering.

The calculated Q-Slope values were utilized to determine the stable slope angles for each location without the need for mechanical support. These stable slope angles were then compared to the actual slope angles observed in field conditions (Fig. 15). The results indicate that only locations L3, L8, and L14 are stable without requiring significant mechanical support. Additionally, seven sites—L1, L4, L6, L9, L10, L11, and L13—are partially stable, as the difference between the actual slope angle and the estimated stable slope angle from Q-Slope is less than 5°, suggesting that minor geometric adjustments may suffice. However, the remaining eight sites have actual slope angles exceeding the estimated stable angles by more than 10°, indicating a high risk of major failure without robust mitigation measures. Location L17 is the most critical, with the actual slope angle exceeding the estimated stable angle by over 30°.

4.6. *Geological Strength Index*

GSI values obtained from field assessments at various locations are categorized into three distinct zones: A, B, and C, within the specific study areas (Fig. 16). Zone A, predominantly features a blocky rock mass that ranges from well-interlocked to intact, with surface conditions that

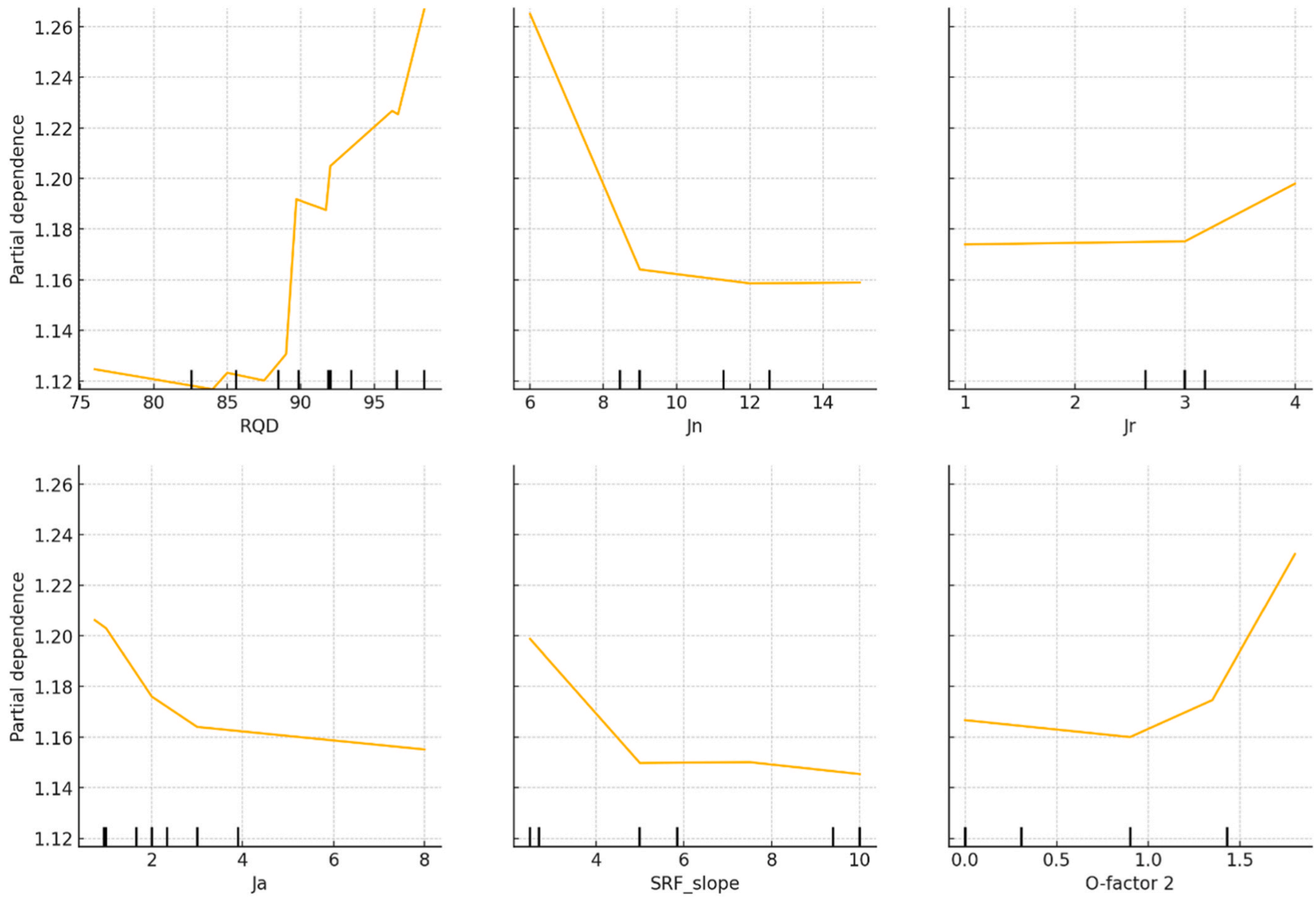

Fig. 14. Partial dependence plot for Q-slope parameters over Q-slope.

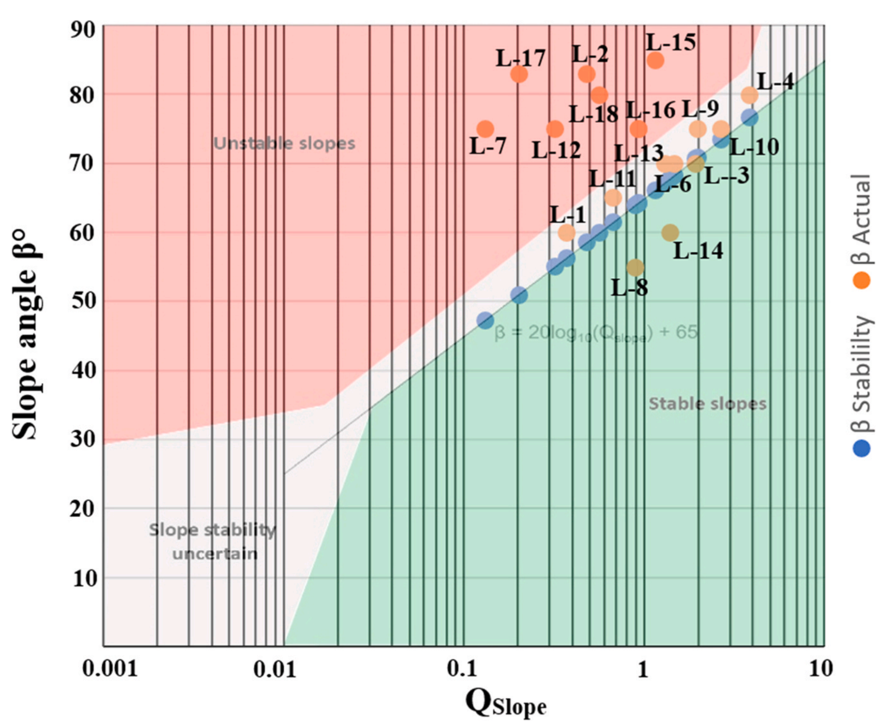

Fig. 15. Comparison of stable slope angle as inferred from Q-Slope with actual slope angles present at studied sites.

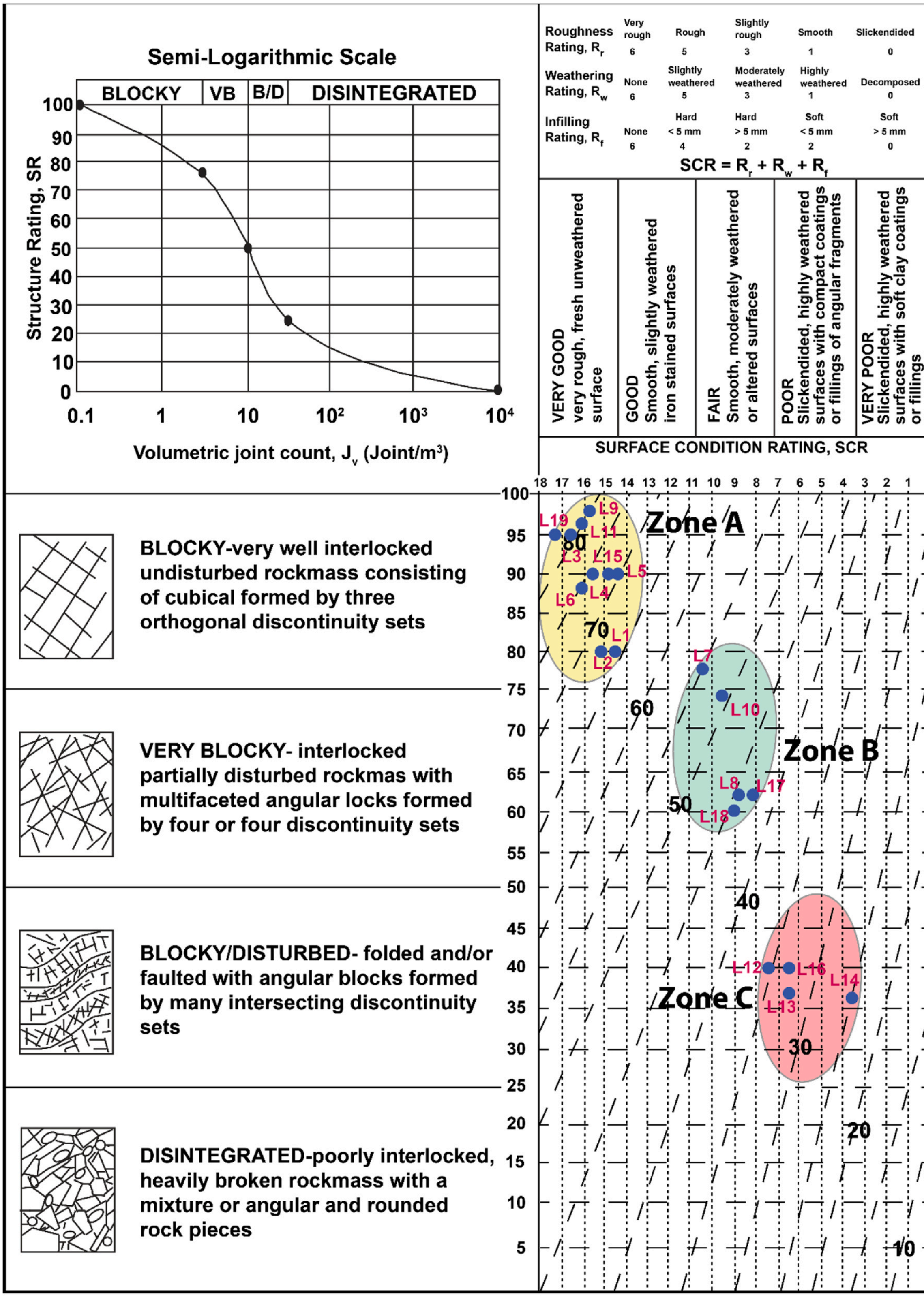

Fig. 16. GSI values at actual ground conditions along the Sangla-Chitkul road at multiple locations examined during field-measurements (after Hoek and Brown 1997).

are fresh to un-weathered. In contrast, Zone B, consists of partially disturbed blocky rock mass with moderately weathered surface conditions. Zone C, is characterized by highly disturbed and angular blocky rock mass, often folded or faulted, with very poor surface conditions marked by slickensides and significant weathering. Overall, the GSI values reveal a trend of decreasing blockiness and surface condition quality from Chitkul to Batseri, transitioning from Zone A to Zone C. This trend correlates with the underlying lithology, where Zone A is predominantly composed of Rakchham granite, known for its significant blockiness, while Zone C consists of gneissic rock, which is more susceptible to weathering. However, a few locations deviate from this pattern mostly due to ongoing tectonic activities and blasting-activities for road construction in the area.

5. Conclusion

The study explores various geomechanical methods of rock-slope condition assessment in Baspa Valley along Sangla-Chitkul road. And, some key empirical approaches adopted in the study are RQD, kinematic analysis, RMR_{basic}, SMR, Q-Slope, and GSI. Furthermore, the field-based datasets are explored for their feature importance and partial dependence relationship with particular classification scheme. Certain schemes are also evaluated for providing a robust stabilization in the area, and the most stable steepest slope angle without any mitigation requirements.

On the basis of RQD, the rock-slopes lies in three classes excellent (61.1 %), good (33.3 %), and fair (5.6 %). In kinematic analysis, single or combined modes of failures were discerned at each studied site, except L3. The feature importance algorithm for RMR_{basic} indicates that RQD, discontinuity spacing, joint conditions are of significant relevance in the study area, with RQD being the top contributor to RMR_{basic}. Germane to RMR_{basic} classification scheme, fifteen out of eighteen, are grouped under Good rockmass condition, and rest belongs to Fair category. In SMR, F3 is the most notable variable with 55.8 % relative importance among all the considered variables in its calculation. Partial dependence analysis highlights the key-role of F3, RQD, and rock strength in effectively improving the SMR rating and mitigation strategy. Eight locations (L1, L6, L7, L8, L11, L14, L16, L17) are partially unstable, and installation of shotcrete, bolt anchors, toe ditches, and nets can enhance slope stability. Locations L2, L3, L9, L10, L12, L13 are in "Good" condition, and a few measures like bolting, anchoring, and fencing could further reduce risk. Also, the sites L5, L15, and L18 fall under the "Very Bad" class, indicating complete instability. Extensive measures, including re-excavation, drainage, shotcrete, and toe walls are needed for robust stabilization.

Two variables J_n and RQD are of utmost significance, while orientation factors (O-1 and O-2), J_a, and J_{wice} have extremely less worth (<10 %) in Q-Slope assessment. Furthermore, the partial dependence analysis shows a marked positive correlation of RQD with Q-Slope ratings, especially for RQD greater than 90 %. Also, examines a pertinent negative impact of J_n, particularly as it varies from 6 to 10. Additionally, a steepest stable slope angle determined using Q-Slope values indicates that only three locations are safe without any additional efforts. The study also includes geological strength index to detailed understanding of rock-slope conditions. The estimated GSI values shows an aggravating rock-slope condition on traversing from Chitkul (L1) to Sangla (L18) along the road, with certain exceptions. The three zones on the basis of GSI-scores are A (65−95), B (45−55), and C (25−35).

All these geomechanical classifications schemes employed in the present study are widely practiced for designing slope geometry and appropriate mitigation implementation. And, their successful amalgamation with feature's importance analysis and PDPs significantly improves the practical importance of present study. Integrating these classifications with feature importance analysis and Partial Dependence Plots (PDPs) enhances the value and relevance of the current study. This integration offers a holistic comprehension of the role each parameter plays in a particular geotechnical classification. The findings contribute to optimizing data collection, identifying key variables, and improving the precision of geomechanical classifications in comparable geo-environmental situations across the globe.

CRediT authorship contribution statement

Kainthola Ashutosh: Writing – review & editing, Supervision, Investigation, Funding acquisition, Conceptualization. **Pandey Vishnu Himanshu Ratnam:** Writing – review & editing, Writing – original draft, Methodology, Investigation, Data curation, Conceptualization. **Kushwaha Gaurav:** Investigation, Formal analysis, Data curation. **Yadav Vikas:** Investigation, Formal analysis, Methodology.

Declaration of Competing Interest

There are no conflicts to declare.

Acknowledgments

AK & VHRP would like to thank Anusandhan National Research Foundation (ANRF) (previously, Science and Engineering Research Board - SERB), India for the grant CRG/2022/002509.

References

[1] A. Trigila, C. Iadanza, C. Esposito, G. Scarascia-Mugnozza, Comparison of Logistic Regression and Random Forests techniques for shallow landslide susceptibility assessment in Giampilieri (NE Sicily, Italy), Geomorphology 249 (2015) 119–136, https://doi.org/10.1016/j.geomorph.2015.06.001.
[2] V.H.R. Pandey, A. Kainthola, V. Sharma, A. Srivastav, T. Jayal, T.N. Singh, Deep learning models for large-scale slope instability examination in Western Uttarakhand, India, Environ. Earth Sci. 81 (2022) 487, https://doi.org/10.1007/s12665-022-10590-8.
[3] X.T. Feng, C.X. Yang, B.G. He, Z.B. Yao, L. Hu, W. Zhang, R. Kong, J. Zhao, Z.B. Liu, X. Bi, Artificial intelligence technology in rock mechanics and rock engineering, Deep Resour. Eng. 1 (2024) 100008, https://doi.org/10.1016/j.deepre.2024.100008.
[4] L. Li, Q. Jiang, Q. Huang, T. Xiang, J. Liu, Advances in stability analysis and optimization design of large underground caverns under high geostress condition, Deep Resour. Eng. 1 (2024) 100113, https://doi.org/10.1016/j.deepre.2024.100113.
[5] J. Liu, X.T. Feng, X.L. Ding, J. Zhang, D.M. Yue, Stability assessment of the Three-Gorges Dam foundation, China, using physical and numerical modeling—Part I: physical model tests, Int. J. Rock. Mech. Min. Sci. 40 (2003) 609–631, https://doi.org/10.1016/S1365-1609(03)00055-8.
[6] W.G. Pariseau, S. Puri, S.C. Schmelter, A new model for effects of impersistent joint sets on rock slope stability, Int. J. Rock. Mech. Min. Sci. 45 (2008) 122–131, https://doi.org/10.1016/j.ijrmms.2007.05.001.
[7] J. Liu, X.T. Feng, X.L. Ding, Stability assessment of the Three-Gorges Dam foundation, China, using physical and numerical modeling—Part II: numerical modeling, Int. J. Rock. Mech. Min. Sci. 40 (2003) 633–652, https://doi.org/10.1016/S1365-1609(03)00056-X.
[8] D.U. Deere, Technical description of rock cores for engineering purposes, Rock. Mech. Eng. Geol. 1 (1964) 17–22.
[9] Z.T. Bieniawski, Engineering classification of jointed rock masses, Trans. S. Afr. Inst. Civ. Eng. 15 (1973) 335–344.
[10] Z.T. Bieniawski, The Geomechanics Classification in Rock Engineering Application. Proceedings 4th International Congress on Rock Mechanics, Montreux, 1979, pp. 41-48.
[11] Z.T. Bieniawski, Engineering rock mass classifications, Wiley, New York, 1989.
[12] M. Romana, New adjustment ratings for application of Bieniawski classification to slopes. In: Proceedings of the International Symposium on Role of Rock Mechanics. Zacatecas, Mexico, 1985, p. 49–53.
[13] M. Romana, A Geomechanical Classification for Slopes: Slope Mass Rating, in: J. A. Hudson (Ed.), Comprehensive Rock Engineering: Principles, Practice and Projects, 3, Pergamon Press, Oxford, 1993, pp. 575–600.
[14] M. Romana, SMR Geomechanics Classification: Application, Experience and Future Development 1995.
[15] N. Barton, R. Lien, J. Lunde, Engineering classification of rock masses for the design of tunnel support, Rock. Mech. 6 (4) (1974) 189–236.
[16] E. Hoek, Strength of rock and rock masses, ISRM N. J. 2 (2) (1994) 4–16.
[17] T.D. Sullivan, Global slope performance index. In Digit PM (ed) Proceedings of slope stability 2013, Brisbane, Australia, 2013, pp. 55–80. ⟨https://doi.org/10.36487/ACG_rep/1308_0.4_Sullivan⟩.
[18] V. Yadav, A. Kainthola, V.H.R. Pandey, G. Kushwaha, T.N. Singh, Discontinuity-Induced Partial Instability in Markundi Hills, Sonbhadra, Uttar Pradesh, India, Geotech. Geol. Eng. 28 (2024) 1–7, https://doi.org/10.1007/s10706-024-02859-5.
[19] P. Lindsay, R.N. Campbell, D.A. Fergusson, G.R. Gillard, T.A. Moore, Slope stability probability classification, Waikato coal measures, New Zealand, Int. J. Coal Geol. 45 (2001) 127–145, https://doi.org/10.1016/S0166-5162(00)00028-8.
[20] J.L. Pastor, A.J. Riquelme, R. Tomás, Clarification of the slope mass rating parameters assisted by SMRTool, an open-source software, Bull. Eng. Geol. Environ. 78 (2019) 6131–6142, https://doi.org/10.1007/s10064-019-01528-9.
[21] S. Andrade, Application of rock mass rating and slope mass rating in slopes of central Portugal, Int Multidiscip. Sci. GeoConf SGEM 21 (2021) 117–128, https://doi.org/10.5593/sgem2021/1.1/s02.021.
[22] M. Azarafza, M.K. Koçkar, H.H. Zhu, Correlations of SMR-Q_{slope} Data in Stability Classification of Discontinuous Rock Slope: A Modified Relationship Considering

the Iranian Data, Geotech. Geol. Eng. 40 (2022) 1751–1764, https://doi.org/10.1007/s10706-021-01991-w.

[23] J. Kundu, K. Sarkar, A.K. Verma, Novel methods for quantitative analysis of kinematic stability and slope mass rating in jointed rock slopes with the aid of a new computer application, Bull. Eng. Geol. Environ. 81 (2022) 29, https://doi.org/10.1007/s10064-021-02524-8.

[24] K. Anbarasu, S. Gupta, A. Sengupta, Site-specific geological and geotechnical studies on the Lanta Khola landslide, North Sikkim Highway, India, Int. J. Geotech. Eng. 3 (2009) 361–376, https://doi.org/10.3328/IJGE.2009.03.03.361-376.

[25] K. Sarkar, T.N. Singh, A.K. Verma, A numerical simulation of landslide-prone slope in Himalayan region—a case study, Arab. J. Geosci. 5 (2012) 73–81, https://doi.org/10.1007/s12517-010-0148-8.

[26] A. Kainthola, V. Sharma, V.H.R. Pandey, T. Jayal, M. Singh, A. Srivastav, P. K. Singh, P.K. Champati-Ray, T.N. Singh, Hill slope stability examination along lower tons valley, Garhwal Himalayas, India, Geomat. Nat. Hazards Risk 12 (2021) 900–921, https://doi.org/10.1080/19475705.2021.1906758.

[27] S. Panthee, S. Dulal, V.H.R. Pandey, V. Yadav, P.K. Singh, A. Kainthola, Engineering geological characteristics and failure mechanics of Jure rock avalanche, Nepal, Geoenviron. Disasters 10 (1) (2023) 25, https://doi.org/10.1186/s40677-023-00256-3.

[28] T.A. Ansari, K.M. Sharma, T.N. Singh, Empirical slope stability assessment along the road corridor NH-7, in the lesser Himalayan, Geotech. Geol. Eng. 37 (2019) 5391–5407, https://doi.org/10.1007/s10706-019-00988-w.

[29] T. Siddique, S.P. Pradhan, V. Vishal, T.N. Singh, Applicability of Q-slope method in the Himalayan Road cut rock slopes and its comparison with CSMR (https://link.springer.com/article/), Rock. Mech. Rock. Eng. 53 (2020) 4509–4522, https://doi.org/10.1007/s00603-020-02176-2.

[30] R. Khanna, R.K. Dubey, Comparative assessment of slope stability along road-cuts through rock slope classification systems in Kullu Himalayas, Himachal Pradesh, India, Bull. Eng. Geol. Environ. 80 (2021) 993–1017, https://doi.org/10.1007/s10064-020-02021-4.

[31] K. Dutta, N. Wanjari, A.K. Misra, Stability analysis of road cut slopes in Sikkim Himalaya along national highway 10, India, Geol. Ecol. Landsc. 2 (2023) 1–4, https://doi.org/10.1080/24749508.2023.2182067.

[32] V.H.R. Pandey, A. Kainthola, T.N. Singh, Empirical and Numerical Evaluation of a Cut Slope Near Rishikesh, India (Singapore). International Conference on Geotechnical Challenges in Mining, Tunneling and Underground Infrastructures; Dec 20, Springer Nature, Singapore, 2021, pp. 579–596, https://doi.org/10.1007/978-981-16-9770-8_38 (Singapore).

[33] A.K. Singh, J. Kundu, K. Sarkar, Stability analysis of a recurring soil slope failure along NH-5, Himachal Himalaya, India, Nat. Hazards 90 (2018) 863–885, https://doi.org/10.1007/s11069-017-3076-z.

[34] A. Kumar, R.K. Sharma, B.S. Mehta, Slope stability analysis and mitigation measures for selected landslide sites along NH-205 in Himachal Pradesh, India, J. Earth Syst. Sci. 129 (2020) 135, https://doi.org/10.1007/s12040-020-01396-y.

[35] K. Singh, V. Kumar, Slope stability analysis of landslide zones in the part of Himalaya, Chamba, Himachal Pradesh, India, Environ. Earth Sci. 80 (8) (2021) 332, https://doi.org/10.1007/s12665-021-09629-z.

[36] V. Kumar, V. Gupta, I. Jamir, S.L. Chattoraj, Evaluation of potential landslide damming: Case study of Urni landslide, Kinnaur, Satluj valley, India, Geosci. Front. 10 (2) (2019) 753–767, https://doi.org/10.1016/j.gsf.2018.05.004.

[37] N. Barton, V. Choubey, The shear strength of rock joints in theory and practice, Rock. Mech. Rock. Eng. 10 (1977) 1–54.

[38] A. Palmstrom, Measurements of and correlations between block size and rock quality designation (RQD), Tunn. Under Space Technol. 20 (4) (2005) 362–377.

[39] C. Edelbro, Rock mass strength – a review. Technical Report, Luleå University of Technology, 2003, p. 132.

[40] S.Y. Choi, H.D. Park, Variation of the rock quality designation (RQD) with scanline orientation and length: a case study in Korea, Int. J. Rock. Mech. Min. Sci. 41 (2004) 207–221, https://doi.org/10.1016/S1365-1609(03)00091-1.

[41] E. Hoek, J.W. Bray. Rock Slope Engineering, 3rd ed., The Institution of Mining and Metallurgy, London, UK, 1981, pp. 341–351.

[42] J. Kundu, K. Sarkar, E. Ghaderpour, G. Scarascia-Mugnozza, P. Mazzanti, A GIS-based kinematic analysis for jointed rock slope stability: an application to Himalayan slopes, Land 12 (2023) 402, https://doi.org/10.3390/land12020402.

[43] W. Ritter, Die Statik der Tunnelgewölbe, Springer, Berlin, 1879.

[44] K. Terzaghi, Rock defects and loads on tunnel supports, in: R.V. Proctor, T.L. White (Eds.), Rock tunneling with steel supports, Commercial Shearing and Stamping Company, Youngstown, OH, 1946, pp. 17–99.

[45] H. Lauffer, Gebirgsklassifizierung für den Stollenbau, Geol. Bauwes. 24 (1) (1958) 46–51.

[46] G.E. Wickham, H.R. Tiedemann, E.H. Skinner, Support determination based on geologic predictions, in: K.S. Lane, L.A. Garfield (Eds.), Proc. North American rapid excav. tunneling conf., Soc. Min. Engrs, Am. Inst. Min. Metall. Petrolm Engrs, Chicago. New York, 1972, pp. 43–64.

[47] F. Pacher, L. Rabcewicz, J. Golser, Zum der seitigen Stand der Gebirgsklassifizierung in Stollen-und Tunnelbau. Proc. XXII Geomech Colloq, Salzburg. 1974, pp. 51-58.

[48] M. Romana, R. Tomas, J.B. Seron, Slope Mass Rating (SMR) Geomechanics Classification: Thirty Years Review. ISRM Congress 2015 Proceedings-International Symposium on Rock Mechanics, Quebec, Canada, 2015, pp. 10.

[49] N. Barton, N. Bar, Introducing the Q-slope method and its intended use within civil and mining engineering projects. In: Schubert W., Kluckner A., editors. Future development of rock mechanics; Proceedings of the ISRM regional symposium, Eurock and 64th geomechanics colloquium, Salzburg, 2015, p. 157–162.

[50] E. Hoek, P. Marinos, M. Benissi, Applicability of the geological strength index (GSI) classification for weak and sheared rock masses—the case of the Athens schist formation, Bull. Eng. Geol. Env. 57 (1998) 151–160, https://doi.org/10.1007/s100640050031.

[51] P. Marinos, E. Hoek, GSI: a geologically friendly tool for rock mass strength estimation. Proceedings of the GeoEng2000 at the international conference on geotechnical and geological engineering, Technomic publishers, Melbourne. Lancaster, 2000, pp. 1422–1444.

[52] P. Marinos, E. Hoek, Estimating the geotechnical properties of heterogeneous rock masses such as flysch, Bull. Eng. Geol. Env. 60 (2001) 82–92, https://doi.org/10.1007/s100640000090.

[53] C. Daniel, A.I. Daniel, Advanced predictive model and feature importance analysis for geological characteristics in tunnelling operations, Discov. Geosci. 2 (2024) 97, https://doi.org/10.1007/s44288-024-00102-5.

[54] C.-H. Hsiao, K. Kumar, E. Rathje, Explainable AI models for predicting liquefaction-induced lateral spreading, Front. Built Environ. (2024), https://doi.org/10.48550/arXiv.2404.15959.

[55] Y. Lin, S. Wang, J. Thiagarajan, G. Guthrie, D. Coblentz, Efficient data-driven geologic feature characterization from pre-stack seismic measurements using randomized machine learning algorithm, Geophys. J. Int. 215 (3) (2018) 1900–1913, https://doi.org/10.1093/gji/ggy385.

[56] R.K. Verma, R. Singh, P. Sharma, T.N. Singh, R.K. Umrao, R.K. Chaurasia, Stability assessment of road-cut slopes along a section of NH-109 in Lesser Kumaun Himalaya, Uttarakhand, India, Nat. Hazards 11 (2024) 1–32, https://doi.org/10.1007/s11069-024-06999-y.

[57] Y. Mao, L. Chen, Y.A. Nanehkaran, M. Azarafza, R. Derakhshani, Fuzzy-based intelligent model for rapid rock slope stability analysis using Qslope, Water 15 (16) (2023) 2949, https://doi.org/10.3390/w15162949.

[58] T. Siddique, Rock mass classification in slope engineering with special emphasis on Slope mass rating: Current status and future projections, Geol. J. (2024), https://doi.org/10.1002/gj.4933.

[59] C.B. Borja, R. Laín, L. Jordá, M. Cano, A. Riquelme, R. Tomás, Stability Assessment of Rock Slopes Using the Q-Slope Classification System: A Reliability Analysis Employing Case Studies in Ecuador, Appl. Sci. 13 (2023) 7399, https://doi.org/10.3390/app13137399.

Ashutosh Kainthola Dr. Kainthola is an Assistant Professor of Engineering Geology in the Department of Geology, Banaras Hindu University, Varanasi, India. His research expertise includes slope stability, machine learning, numerical modelling, tunneling, geohazards, and geotechnical engineering. He has extensive experience working in industry and academia.

Vishnu Himanshu Ratnam Pandey Mr. Pandey is a research scholar in the Department of Geology, Banaras Hindu University, Varanasi, India. He is currently working on rock slope instability assessment in the Higher Himalayan condition. His work include numerical modeling and machine learning in comprehension of slope instability and landslides.

Gaurav Kushwaha Mr. Kushwaha is a research scholar in the Department of Geology, Banaras Hindu University, Varanasi, India. Area of his research interests are empirical methods, remote sensing and GIS, landslide, societal impact of geohazards.

Vikas Yadav Mr. Yadav is research scholar in the Department of Geology, Banaras Hindu University, Varanasi, India. His research interests include rock mechanics, underground excavation, and geohazard assessment.